JACS
JOURNAL OF THE AMERICAN CHEMICAL SOCIETY

COMMUNICATION

pubs.acs.org/JACS

Iridium N-Heterocyclic Carbene Complexes as Efficient Catalysts for Magnetization Transfer from *para*-Hydrogen

Michael J. Cowley,[†] Ralph W. Adams,[†] Kevin D. Atkinson,[†] Martin C. R. Cockett,[†] Simon B. Duckett,[†,*] Gary G. R. Green,[‡] Joost A. B. Lohman,[§] Rainer Kerssebaum,[∥] David Kilgour,[∥] and Ryan E. Mewis[†]

[†]Department of Chemistry, University of York, Heslington, York YO10 5DD, U.K.

[‡]York Neuroimaging Centre, The Biocentre, York Science Park, Heslington, York YO10 5DG, U.K.

[§]Bruker U.K., Limited, Banner Lane, Coventry CV4 9GH, U.K.

[∥]Bruker BioSpin GmbH, Silberstreifen 4, 76287 Rheinstetten, Germany

Supporting Information

ABSTRACT: While the characterization of materials by NMR is hugely important in the physical and biological sciences, it also plays a vital role in medical imaging. This success is all the more impressive because of the inherently low sensitivity of the method. We establish here that $[Ir(H)_2(IMes)(py)_3]Cl$ undergoes both pyridine (py) loss as well as the reductive elimination of H_2. These reversible processes bring *para*-H_2 and py into contact in a magnetically coupled environment, delivering an 8100-fold increase in ^1H NMR signal strength relative to non-hyperpolarized py at 3 T. An apparatus that facilitates signal averaging has been built to demonstrate that the efficiency of this process is controlled by the strength of the magnetic field experienced by the complex during the magnetization transfer step. Thermodynamic and kinetic data combined with DFT calculations reveal the involvement of $[Ir(H)_2(\eta^2\text{-}H_2)(IMes)(py)_2]^+$, an unlikely yet key intermediate in the reaction. Deuterium labeling yields an additional 60% improvement in signal, an observation that offers insight into strategies for optimizing this approach.

NMR finds widespread use in chemistry, biochemistry, and medicine in spite of its inherently low sensitivity, which arises from the small energy difference between the nuclear spin state orientations it probes.[1,2] This is the case because the magnitude of the net polarization in the direction of the applied magnetic field is proportional to the population difference between the addressed nuclear spin states. Hyperpolarization techniques redistribute the nuclear spin state populations to provide greatly enhanced sensitivity.[3,4] Dynamic nuclear polarization (DNP),[5] which employs polarization transfer from an unpaired electron at low temperature (1.3 K) over the course of several hours, is one of the most successful approaches to hyperpolarization. A good example of the power of this approach has been demonstrated in its use to increase the level of ^{13}C polarization for the C1 site in pyruvic acid to 64%.[6] An alternative approach incorporates *para*-H_2[7] into a molecule to produce products containing nonequilibrium nuclear spin state populations.[8,9] Such products can produce hyperpolarized NMR signals for which the detected response derives from only a single populated energy level.[10] The impact that this approach is already having in preclinical research illustrates the huge potential that such signal improvements can have in studying disease.[11−13]

In a recent development, polarization transfer from *para*-H_2 was achieved over much shorter time scales (∼seconds) than for DNP without the need to incorporate it into the molecule of interest.[14] This involved the reaction of Crabtree's catalyst, $[Ir(COD)(PCy_3)(py)][BF_4]$ (COD = cyclooctadiene; Cy = cyclohexyl),[15] with both py and *para*-H_2 to form the polarization transfer catalyst $[Ir(H)_2(PCy_3)(py)_3][BF_4]$ (**1**$[BF_4]$).[16] Such signal amplification by reversible exchange (SABRE) in a low magnetic field results in transfer of the nuclear spin order from *para*-H_2 to free py, with >100-fold signal enhancements observed in ^1H, ^{13}C, and ^{15}N NMR spectra. SABRE has also been used in trace-component analysis at low fields.[17]

It has been predicted theoretically that the hyperpolarization efficiency of SABRE depends on both the lifetime of the metal complex and the strength of the magnetic field in which polarization transfer occurs.[18] Earlier experimental studies demonstrated that sterically bulky electron-donating phosphines, such as PCy_3, deliver the highest levels of transferred hyperpolarization.[16] Even greater efficiencies might therefore be expected with a strongly electron-donating N-heterocyclic carbene (NHC) ligand;[19] related carbene complexes have been used as hydrogenation catalysts.[20] Using purpose-built apparatus, we have shown in the present work that $[IrCl(COD)(IMes)]$ (**2**)[21] [IMes = 1,3-bis(2,4,6-trimethylphenyl)imidazole-2-ylidene[22]] is a much better SABRE catalyst than **1**. This has also allowed us to test the earlier theoretical predictions.[18]

After treatment of **2** with excess py in methanol, $[Ir(COD)(IMes)(py)]Cl$ (**3**[Cl]) was produced. When solutions of **3**[Cl] were exposed to H_2, they became colorless in minutes. NMR spectroscopy and mass spectrometry confirm that $[Ir(H)_2(IMes)(py)_3]Cl$ (**4**[Cl]) has been formed (Scheme 1). The X-ray structure of **4**$[PF_6]$, (Figure 1), shows distorted octahedral complex, with two mutually cis hydride ligands located in the same plane as two mutually cis py ligands. This structure is similar to that of $[Ir(H)_2(IMes)(NCMe)_3]BF_4$ determined by Solar et al.[23]

Received: January 26, 2011
Published: April 06, 2011

dx.doi.org/10.1021/ja200299u | *J. Am. Chem. Soc.* 2011, 133, 6134–6137

Scheme 1. Formation of 3[Cl] and 4[Cl] from 2

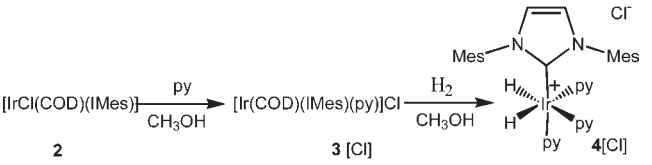

Comparison of the X-ray structures of NHC-containing **4**[PF_6] and the closely related PCy_3 complex **1**[BF_4] reveal that the equatorial and axial Ir−N bond lengths differ by less than 0.01 Å. However, when a solution of $\mathbf{4}^+$ containing 0.06 mmol of py (5 mol % catalyst loading) and 3 atm *para*-H_2 was examined after polarization transfer in the earth's magnetic field (0.5×10^{-4} T), the signal deriving from the meta protons of free pyridine, detected through a simple 90° read pulse, increased by a factor of 266 relative to a thermally polarized sample at 295 K and 9.4 T. This compares with an 18-fold increase for comparable concentrations of $\mathbf{1}^+$, py and *para*-H_2, albeit at 318 K. Thus, in spite of the similar structural parameters, **4**[Cl] is a better magnetization transfer catalyst than **1**[BF_4].

An increase in temperature of solutions containing pyridine, **1**[BF_4], and *para*-H_2 from 295 to 318 K resulted in *increased* polarization transfer to py. In contrast, warming a similar sample of **4**[Cl] *reduced* the level of signal enhancement relative to that at 295 K. It therefore appears that an optimal ligand exchange rate for the polarization transfer step exists.

In order to explore the hyperpolarization transfer process in more detail, a series of ^{1}H EXSY NMR experiments were performed to quantify the free/bound py and hydride/H_2 exchange processes undergone by $\mathbf{4}^+$. An Eyring plot of the rate data for dissociation of a py *trans* to either of the hydride ligands yielded the values $\Delta H^{\ddagger} = 93 \pm 3$ kJ mol^{-1} and $\Delta S^{\ddagger} = 97 \pm 9$ J K^{-1} mol^{-1}. These give $\Delta G^{\ddagger}(300\ \mathrm{K}) = 64 \pm 2$ kJ mol^{-1} deriving from the measured experimental rate constant of 11.7 s^{-1}. The analogous rate constant for py exchange in $\mathbf{1}^+$ is only 1.8 s^{-1}.[16]

In order to better understand these experimental observations, a number of pathways leading to py exchange were examined using density functional theory (DFT). Optimizations of reactant $\mathbf{4}^+$ conducted at the BP86/LANL2DZ level of theory resulted in structures with geometrical parameters very close to those determined from the experimental X-ray crystal structure (see the Supporting Information.). These calculations revealed that loss of the py *trans* to IMes in $\mathbf{4}^+$ results in the same dissociative product after reorganization as that resulting from loss of a py *trans* to hydride (see Figure 1). EXSY data showed that the former does not occur on the NMR timescale. The computed gas-phase free-energy barrier for loss of py *trans* to hydride is 48 kJ mol^{-1}, which compares with the experimental value of 64 ± 2 kJ mol^{-1}. The positive experimental $\Delta S^{\ddagger}$ value for this process indicates a dissociative mechanism, which is further supported by the fact that increasing the py concentration did not significantly alter the observed exchange rate. The larger py exchange rate constant for $\mathbf{4}^+$ than for $\mathbf{1}^+$ may explain the increased hyperpolarization level, but as polarization comes from the hydride ligands, the H_2 exchange rate must be considered.

The H_2-loss pathway in $\mathbf{4}^+$ was monitored by EXSY methods in a manner similar to that for py. At 300 K, the experimentally determined rate constant for H_2 loss is 9 s^{-1}. The associated Eyring plot yielded the values $\Delta H^{\ddagger} = 79 \pm 1$ kJ mol^{-1}, $\Delta S^{\ddagger} = 41 \pm 3$ J K^{-1} mol^{-1}, and $\Delta G^{\ddagger}(300\ \mathrm{K}) = 66.4 \pm 0.3$ kJ mol^{-1}.

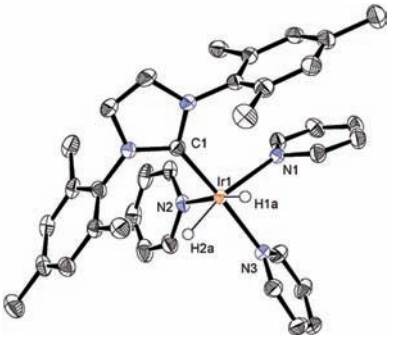

Figure 1. ORTEP plot of **4**[PF_6]·MeOH with ellipsoids at 50% probability; H atoms, the PF_6^- ion, and solvent MeOH have been omitted for clarity. Selected bond lengths (Å) and angles (deg): C1−Ir1, 1.989(3); Ir1−N1, 2.220(3); Ir1−N2, 2.192(3); Ir1−N3, 2.129(3); C1−Ir1−N3, 173.55(12); C1−Ir1−N2, 93.89(12); C1−Ir1−N1, 102.17(12); N3−Ir1−N1, 83.10(11); N2−Ir1−N1, 96.80(11).

These values are substantially different from those for py loss and relate to the overall process by which H_2 elimination occurs, whether that be as a simple concerted loss of H_2 from $\mathbf{4}^+$ or as a multistep sequential process involving other ligand exchange. The rate constant for H_2 loss from $\mathbf{4}^+$ ($k_{\mathrm{obs\text{-}H_2}}$) decreases with increasing py concentration, which, when taken in conjunction with its higher free-energy barrier, suggests that its rate-determining step occurs after py dissociation. However, as $k_{\mathrm{obs\text{-}H_2}}$ also increases with increasing H_2 pressure, H_2 addition must also be involved. Consequently, an exchange pathway involving H_2 loss directly from $\mathbf{4}^+$ can be excluded.

A number of additional routes to H_2 exchange following py loss from $\mathbf{4}^+$ were explored using DFT. The first of these involves formation of an 18-electron H_2 addition complex, $[Ir(H)_4(IMes)(py)_2]Cl$, from $[Ir(H)_2(IMes)(py)_2]Cl$. The DFT calculations showed that while formation of this complex is facile, liberating 11 kJ mol^{-1} of free energy via a free-energy barrier of 27 kJ mol^{-1}, it exists exclusively as the $[Ir(H)_2(\eta^2\text{-}H_2)(IMes)(py)_2]^+$ isomer, where the second H_2 ligand binds in the faster-relaxing dihydrogen form. This process involves a combined gas-phase free-energy barrier of 44 kJ mol^{-1} starting from $\mathbf{4}^+$. This pathway would require the $[Ir(H)_2(\eta^2\text{-}H_2)(IMes)(py)_2]^+$ intermediate to have a lifetime short enough to avoid the conversion of *para*-H_2 to *ortho*-H_2.[24] Computed structures and a free-energy diagram are shown in Figure 2 for this pathway, with the relative Gibbs free energies listed in Table 1. A second route involving the same py-loss intermediate, $[Ir(H)_2(IMes)(py)_2]Cl$, involves simple dihydride elimination and the formation of the 14-electron species $[Ir(IMes)(py)_2]Cl$. The DFT calculations suggest that while such an intermediate would be stable, its formation would be thermodynamically unfavorable, requiring at least 117 kJ mol^{-1} of free energy. This route is inconsistent with the experimental kinetic data. A third route involves explicit solvent participation and the formation of the 18-electron intermediate $[Ir(H)_2(IMes)(py)_2(MeOH)]Cl$. The calculations suggested that while methanol would easily bind to the py-loss product, requiring just 13 kJ mol^{-1} of free energy, subsequent elimination of the dihydride ligands would require an additional 83 kJ mol^{-1}. These latter two pathways are therefore inconsistent with experiment.

The importance of the concentration of H_2 on the polarization transfer process is reflected by the fact that the level of enhancement in the ortho proton signal of free py after reaction in the earth's magnetic field, increased from a factor of 39 at 1 atm *para*-

dx.doi.org/10.1021/ja200299u | J. Am. Chem. Soc. 2011, 133, 6134–6137

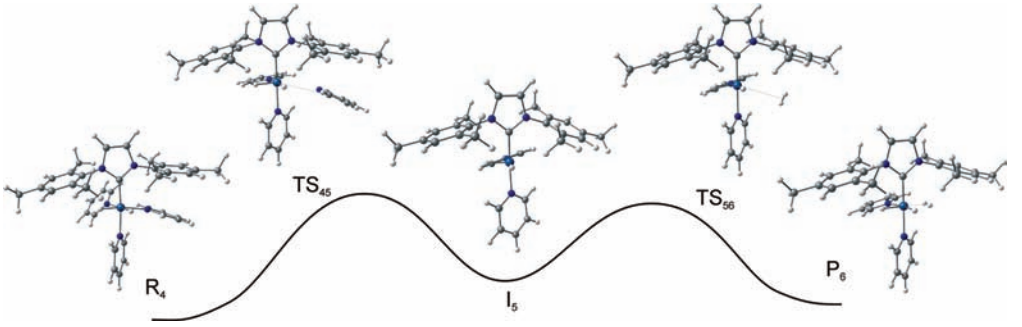

Figure 2. Computed structures and schematic free-energy diagram for pyridine and H_2 exchange in **4**[Cl] at 300 K determined using a combination of vibrational frequency calculations (BP86/LANL2DZ level) and single-point calculations (TPSSTPSS/LANL2DZ/aug-cc-pVDZ level).

Table 1. Relative Gibbs Free Energies (kJ mol^{-1}) for the Species Involved in py and H_2 Exchange in 4[Cl] at 300 K As Shown in Figure 2

$\Delta G^{\ddagger}_{45}$	$\Delta G^{\ddagger}_{54}$	ΔG_{45}	$\Delta G^{\ddagger}_{56}$	$\Delta G^{\ddagger}_{65}$	ΔG_{56}
48	31	17	27	38	−11

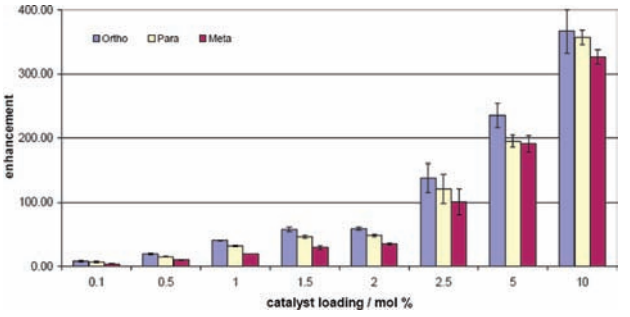

Figure 3. The graph shows the enhancement levels for the three ^{1}H resonances of free-py as a function of catalyst loading, observed after polarization transfer at 0.5 × 10^{-4} T via **4** and 3 atm *para*-H_2.

H_2 to 243 at 3 atm. In a further series of experiments, the catalyst loading was varied from 0.1 to 10 mol % (see Figure 3). These experiments revealed that the enhancements for all three proton sites of free py reached a maximum at a catalyst loading of 10 mol %, at which point the signal deriving from the ortho proton was enhanced by a factor of 360 (1.16% hyperpolarized). At loadings beyond this point, the solution was saturated in **4**[Cl].

Figure 4 illustrates how a reaction cell and flow probe were integrated into the NMR spectrometer to allow the study of both the sample hyperpolarization level and the created nuclear spin states. This setup allowed a sample to be hyperpolarized in a predefined magnetic field prior to monitoring in the spectrometer. For py, the dominant nuclear spin states that survived introduction into the spectrometer were predicted to be of either longitudinal (I_z) or longitudinal two-spin order type (I_zS_z).[18] This apparatus also provided the opportunity for signal averaging on a 20 s time scale (completing steps 1 to 4), an approach which is currently not possible for solution-state DNP. A ^{13}C-INADEQUATE spectrum showing signals for the ortho and meta carbons of 4-picoline, with a common 54 Hz $J_{^{13}C-^{13}C}$ splitting, was obtained in 4 scans using this apparatus.

Two readout methods were used to distinguish between the I_z and I_zS_z states. The first used a 90° read pulse to detect I_z

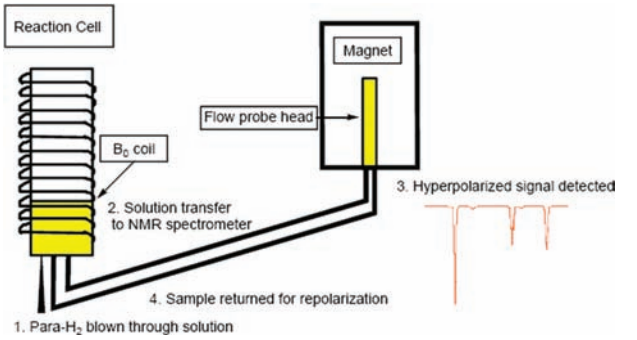

Figure 4. Schematic diagram of the automized hyperpolarized sample preparation process featuring an external reaction cell an NMR flow probe, and a B_0 polarization coil.

magnetization and revealed a maximum response when the sample was exposed to a magnetic field of 70 × 10^{-4} T. The second method selectively detected the longitudinal two-spin magnetization using the OPSY[25] protocol. This transfer yielded a maximum response when carried out close to zero field. These data therefore confirm that this hyperpolarization transfer method does indeed generate the two types of spin states predicted,[18] as illustrated in Figure 5.

The results of this systematic study enabled us to increase the hyperpolarization transfer efficiency to the point where it delivers a 6000-fold ^{1}H signal enhancement for py at 3 T in an MRI system. While this equates to a net polarization level of 6%, the individual ortho, meta, and para proton sites have I_z polarizations of 7.2, 3.8, and 8.1% (8100-fold enhancement), respectively. A potential way to increase the level of polarization further is to use a substrate with fewer protons. In a subsequent experiment with 3,4,5-trideuteriopyridine, having only two ^{1}H spins, a further 60% increase in I_z polarization was observed. Theoretically, this approach should yield 11.5% ^{1}H I_z polarization.[26]

In conclusion, we have demonstrated that [IrCl(COD)(IMes)] (**2**) is a much more efficient magnetization transfer catalyst for the sensitization of pyridyl-based heteroaromatic systems than [IrCl(COD)(PCy$_3$)].[14,16] The key to this process involves bringing *para*-H_2 and the substrate, py, into spin−spin contact, in this case via [Ir(H)$_2$(IMes)(py)$_3$]Cl (**4**[Cl]). The level of hyperpolarization is critically dependent on the py and H_2 exchange rate constants, the reagent concentrations, and the strength of the magnetic field in which the polarization is transferred. Optimization of these parameters yielded an I_z hyperpolarization level of 8.1% for the para proton of py. The hyperpolarization level has been shown to be dramatically

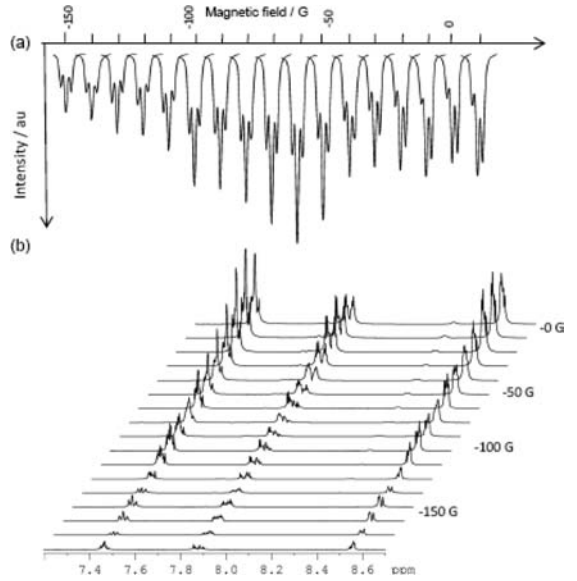

Figure 5. ^{1}H NMR signal response profiles of pyridine measured as a function of the external polarization field (Gauss) for (a) the para site, which shows longitudinal magnetization, and (b) longitudinal two-spin order terms spanning the three sites.

increased when it is shared across fewer proton. In this case, 3,4,5-trideuteriopyridine delivered a 60% improvement in the ortho ^{1}H polarization level. A further benefit of ^{2}H labeling is to extend the lifetime of the created nuclear spin states.[27,28] The appropriate combination of magnetic field, reagent concentrations, and ^{2}H labeling is therefore necessary to maximize the hyperpolarization level using this method.

The DFT and kinetic studies detailed here suggest that the process of H_2 exchange involves $[Ir(H)_2(\eta^2\text{-}H_2)(IMes)(py)_2]^+$ and must occur sufficiently rapidly to offset the fact that H_2 is bound in its faster-relaxing form.

The use of a specially developed reaction cell has been shown to enable signal averaging and the rigorous demonstration that a mixture of longitudinal and longitudinal two-spin order polarization is created at each polarization transfer field through this process. In NMR spectroscopy, the controlled generation of magnetic states is normally achieved through the application of radiofrequency pulses and magnetic field gradient cascades. Here it has been achieved simply by controlling the magnetic field during polarization transfer. This observation has implications for MRI measurements, where the analytes need to be monitored against a high water background because multiple quantum filtration sequences enable H_2O signals to be removed.[29] We are exploring whether the detected longitudinal two-spin order terms are associated with long-lived magnetic states.[30,18]

■ ASSOCIATED CONTENT

Supporting Information. Synthesis details; rate, DFT, and NMR data; and equipment details. This material is available free of charge via the Internet at http://pubs.acs.org.

■ AUTHOR INFORMATION

Corresponding Author
sbd3@york.ac.uk

■ ACKNOWLEDGMENT

We are grateful for financial support from the EPSRC, the MRC, and Bruker BioSpin and for help from Dr. S. Johnson, Dr. D. Williamson, and Dr. M. Hymers.

■ REFERENCES

(1) Wüthrich, K. *Angew. Chem., Int. Ed.* **2003**, *42*, 3340.
(2) Ernst, R. R. *Angew. Chem., Int. Ed. Engl.* **1992**, *31*, 805.
(3) Viale, A.; Aime, S. *Curr. Opin. Chem. Biol.* **2010**, *14*, 90.
(4) Rizi, R. R. *Proc. Natl. Acad. Sci. U.S.A.* **2009**, *106*, 5453.
(5) Ardenkjaer-Larsen, J. H.; Fridlund, B.; Gram, A.; Hansson, G.; Hansson, L.; Lerche, M. H.; Servin, R.; Thaning, M.; Golman, K. *Proc. Natl. Acad. Sci. U.S.A.* **2003**, *100*, 10158.
(6) Johanneson, H.; Macholl, S.; Ardenkjaer-Larsen, J. H. *J. Magn. Reson.* **2009**, *197*, 167.
(7) Bowers, C. R.; Weitekamp, D. P. *J. Am. Chem. Soc.* **1987**, *109*, 5541.
(8) Bhattacharya, P.; Chekmenev, E. Y.; Perman, W. H.; Harris, K. C.; Lin, A. P.; Norton, V. A.; Tan, C. T.; Ross, B. D.; Weitekamp, D. P. *J. Magn. Reson.* **2007**, *186*, 150.
(9) Duckett, S. B.; Wood, N. J. *Coord. Chem. Rev.* **2008**, *252*, 2278.
(10) Blazina, D.; Duckett, S. B.; Halstead, T. K.; Kozak, C. M.; Taylor, R. J. K.; Anwar, M. S.; Jones, J. A.; Carteret, H. A. *Magn. Reson. Chem.* **2005**, *43*, 200.
(11) Johansson, E.; Mansson, S.; Wirestam, R.; Svesson, J.; Petersson, S.; Golman, K.; Stahlberg, F. *Magn. Reson. Med.* **2004**, *51*, 464.
(12) Terreno, E.; Castelli, D. D.; Viale, A.; Aime, S. *Chem. Rev.* **2010**, *110*, 3019.
(13) Ross, B. D.; Bhattacharya, P.; Wagner, S.; Tran, T.; Sailasuta, N. *Am. J. Neuroradiol.* **2010**, *31*, 24.
(14) Adams, R. W.; Aguilar, J. A.; Atkinson, K. D.; Cowley, M. J.; Elliott, P. I. P.; Duckett, S. B.; Green, G. G. R.; Khazal, I. G.; Lopez-Serrano, J.; Williamson, D. C. *Science* **2009**, *323*, 1708.
(15) Crabtree, R. H.; Lavin, M.; Bonneviot, L. *J. Am. Chem. Soc.* **1986**, *108*, 4032.
(16) Atkinson, K. D.; Cowley, M. J.; Elliott, P. I. P.; Duckett, S. B.; Green, G. G. R.; Lopez-Serrano, J.; Whitwood, A. C. *J. Am. Chem. Soc.* **2009**, *131*, 13362.
(17) Gong, Q. X.; Gordji-Nejad, A.; Blumich, B.; Appelt, S. *Anal. Chem.* **2010**, *82*, 7078.
(18) Adams, R. W.; Duckett, S. B.; Green, R. A.; Williamson, D. C.; Green, G. G. R. *J. Chem. Phys.* **2009**, *131*, No. 194505 (doi:10.1063/1.3254386).
(19) Diez-Gonzalez, S.; Nolan, S. P. *Coord. Chem. Rev.* **2007**, *251*, 874.
(20) Vazquez-Serrano, L. D.; Owens, B. T.; Buriak, J. M. *Chem. Commun.* **2002**, 2518.
(21) Vazquez-Serrano, L. D.; Owens, B. T.; Buriak, J. M. *Inorg. Chim. Acta* **2006**, *359*, 2786.
(22) Bourissou, D.; Guerret, O.; Gabbai, F. P.; Bertrand, G. *Chem. Rev.* **2000**, *100*, 39.
(23) Torres, O.; Martín, M.; Sola, E. *Organometallics* **2009**, *28*, 863.
(24) Thomas, A.; Haake, M.; Grevels, F. W.; Bargon, J. *Angew. Chem., Int. Ed. Engl.* **1994**, *33*, 755.
(25) Aguilar, J. A.; Elliot, P. I. P.; López-Serrano, J.; Adams, R.; Duckett, S. B. *Chem. Commun.* **2007**, 1183.
(26) When a sample of optimum reagent concentrations was prepared to test this, the receiver was saturated on the lowest setting.
(27) Chekmenev, E. Y.; Hovener, J.; Norton, V. A.; Harris, K.; Batchelder, L. S.; Bhattacharya, P.; Ross, B. D.; Weitekamp, D. P. *J. Am. Chem. Soc.* **2008**, *130*, 4212.
(28) Reineri, F.; Santelia, D.; Gobetto, R.; Aime, S. *J. Magn. Reson.* **2009**, *200*, 15.
(29) Thompson, R. B.; Allen, P. S. *Magn. Reson. Med.* **2009**, *62*, 796.
(30) Carravetta, M.; Levitt, M. H. *J. Am. Chem. Soc.* **2004**, *126*, 6228.